Date of publication xxxx 00, 0000, date of current version xxxx 00, 0000.

Digital Object Identifier 10.1109/ACCESS.2019.DOI

An Accurate Analytical Model to Calculate the Impedance Bandwidth of a Proximity Coupled Microstrip Patch Antenna (PC-MSPA)

NAFATI ABOSERWAL[1,2], (Member, IEEE), NIM CCOILLO-RAMOS[1,2], (Student Member, IEEE), ZEESHAN QAMAR[1,2], (Member, IEEE), and JORGE L. SALAZAR-CERRENO[1,2], (Senior Member, IEEE)

[1]Advanced Radar Research Center (ARRC), The University of Oklahoma, Norman, OK 73019 USA.
[2]School of Electrical and Computer Engineering, The University of Oklahoma, Norman, OK 73019 USA.

Corresponding author: Jorge L. Salazar-Cerreno (e-mail: salazar@ou.edu)

ABSTRACT This paper presents a new set of analytical equations to calculate the impedance bandwidth of electrically thin and thick proximity-coupled square microstrip patch antenna (PC-MSPA). The proposed mathematical model uses the relationship among different antenna parameters, material, and antenna dimensions to estimate the percentage impedance bandwidth with high accuracy. The proposed model was validated with rigorous full-wave solutions, and experimental antenna prototypes implemented for different thicknesses, patch dimensions, frequencies, and different substrates. The theoretical bandwidth results of S-, C- and X-band PC-MSPA antennas obtained using the new model are in very good agreement with simulations and the experimental results. Errors between the proposed analytical model and both simulation and measurement are less than 3.1%. These equations are mostly valid for permittivities between 2.2 and 6.15, and with feed substrate thickness less than $0.1\lambda_r$. The PC-MSPA is a candidate element for integration with MMIC devices and wireless communication applications.

INDEX TERMS microstrip patch antenna, proximity coupling feed, wide bandwidth, multi-layer structure, non-linear curve-fitting technique.

I. INTRODUCTION

MICROSTRIP patch antennas were first proposed by Deschamps in 1953 [1] and patented by Gutton and Baissinot in 1955 [2]. However, practical microstrip patch antennas were developed by Munson [3] and Howell [4] in the 1970s. Microstrip patch antennas have several well-known advantages over other conventional antennas; low cost, light weight, ease of manufacture, rugged, low radar cross-section, conformability, low production cost, compatibility with microwave integrated circuits, and capability to be easily formed into arrays [5]–[8]. These advantages make the microstrip patch antennas suitable for high performance aircraft, missiles, radars, satellite and mobile communication, radio frequency identification (RFID), global positioning system, space craft, and biomedical applications. However, a well-known inherent disadvantage of microstrip patch antennas is their narrow impedance bandwidth that is typically a few percent because they are highly resonant structures. One of the important aspects of microstrip patch antennas is the variety of feeding techniques applicable to them. The comparison between those common feeding techniques is presented in [5]–[8]. The PC-MSPA is one of the printed antennas that provide a broadband, efficient solutions to integrating antennas with MIMIC circuits.

The proximity-coupled feeding technique, one of non-contact feeding methods, provides large bandwidth (as high as 13%) compared to other feeding techniques where there is a direct contact between the feed line and the radiating patch like a probe-fed and edge-fed methods [5]–[8]. In contrast to the direct contact methods, which are predominantly inductive, this feeding mechanism is capacitive in nature. This capacitive loading significantly affects the obtained impedance bandwidth, thus providing a wider bandwidth. In addition, this simple feeding technique provides enhanced

bandwidth without undesired radiation caused by the discontinuities and asymmetry of direct contact feed methods [5]–[8].

The modeling and analysis of a proximity-coupled microstrip patch antenna is difficult due to the complex electromagnetic interaction involved between the feed line and the radiating patch. Over the past decades, microstrip patch antennas have been analyzed extensively, employing a wide variety of analytical techniques, which are simple intuitive models with different levels of approximation as the transmission line model, the cavity model and segmentation model [9]–[13]. These models work well for thin, low dielectric constant substrate, but exhibit less accuracy at the substrate thickness and/or the dielectric constant increases. Some of the feed configurations such as proximity-coupled microstrip feed is difficult to model using the analytical techniques because the effect of the coupling capacitor between the microstrip feed line and the patch as well as the equivalent R-L-C resonant circuit representing the patch with two-layered substrate should be taken into account when designing the antenna. However, most of the analytical models' limitations can be overcome in the full-wave techniques. In [14]–[17], the most popular full-wave techniques such as the method of moments (MoM), the finite-element method (FEM), the spectral domain technique (SDT), the finite-difference time domain (FDTD) method have been used to analyze and design a proximity-coupled microstrip patch antenna. Although these numerical techniques maintain accuracy, completeness and versatility at the expense of numerical simplicity, they are difficult to implement due to extensive computational procedures.

In [18], graphical guidelines for design of proximity-coupled square and circle microstrip patch antennas are given. These graphical design curves are obtained by using a rigorous moment method formulation, employing the Green function for the double-layered structure. To the authors knowledge, there appears to be no overview on how to achieve broad impedance bandwidth for a double-layered proximity-coupled microstrip patch antenna and how its parameters affects the antenna bandwidth.

This paper proposes a mathematical-based analysis and a alternative design procedure that provides a solution for a PC-MSPA design. Therefore, the organization of this paper is as follows: A brief review of PC-MSPA is presented in Section II . Then, in Section III, described the proposed model in detail. In Section IV, four antenna prototypes were developed and tested to validate the proposed model. Section V, shows an error analysis of proposed model and comparison with other analytical expressions used for bandwidth estimation of conventional MS patch antennas.

II. PROXIMITY-COUPLED MICROSTRIP PATCH ANTENNA (PC-MSPA)

The double-layered proximity-coupled square microstrip patch antenna shown in Fig. 1 is called electromagnetically coupled (EMC) microstrip patch antenna. This type of

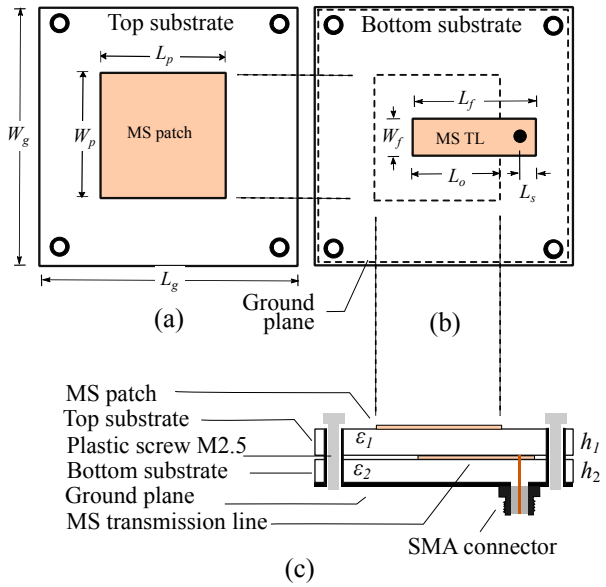

FIGURE 1: Geometry of the proximity-coupled square microstrip patch antenna (PC-MSPA). (a) Top view. (b) Mid-section of PC-MSPA, and (c) Stack-up definition of PC-MSPA.

feeding technique comes under non contacting scheme as there is no physical contact between the radiating patch and the feed line. As shown in Fig. 1, two substrates are used such that the feed line terminated with an open circuit is between the two substrates, the radiating patch with dimensions L_p and W_p is on top of the upper substrate and the lower (feed) substrate is grounded. The microstrip feedline of width W_f is centered with respect to the patch width, and is inset a distance L_0 from the the edge of the patch.

Since no direct contact between the microstrip feed line and the radiating patch in this feeding mechanism, the radiating patch on the upper substrate (patch layer) is excited by an open-ended microstrip feed line printed on the lower substrate (feed layer) through capacitive coupling. Matching can be achieved by controlling the length of the feed line (feeding stub) and the width-to-line ratio of the patch. The coupling increases with feed inset reaching a maximum when L_0=$L_p/2$. The coupling is symmetrical with respect to the center of the patch and can be increased by decreasing the patch width [19].

The main advantage of this feed technique is that it provides high bandwidth and eliminates spurious feed radiation, due to overall increase in the thickness of the microstrip patch antenna. In addition, this technique gives option to independently select the two dielectric substrates to further optimize both feed line performance and patch performance. However, the fabrication is bit complex which is a disadvantage.

Different approaches have been found in the state of technique that aims to analyze and optimize different parameters of microstrip patch antennas, such as the bandwidth, the cross-polarization level and the gain, based on full-wave

solutions. Apart of the simulation-based techniques, two-layer PC-MSPA modeling has been approached in the state of art, although its challenges and limited close models available so far. Considering the average permittivity [20] and its effective value, Parrikar and Gupta [21] developed a multi-port model making the two substrates be equivalent to a one-average substrate, which average electrical relative permittivity was calculated as follows:

$$\varepsilon_{av} = \frac{\varepsilon_1\varepsilon_2(h_1+h_2)}{\varepsilon_1 h_2 + \varepsilon_2 h_1} \quad (1)$$

Besides, diverse studies have analyzed the microstrip patch antenna with different feeding strategies, seeking for an analytical expression of the bandwidth. Starting from different expressions of the bandwidth based on the VSWR [22], [23], Jackson and Alexopoulos [24] derived a closed form of the bandwidth for one-substrate microstrip patch antennas. This formula becomes increasingly inaccurate for thicker or multiple substrates. A different expression for calculating the percentage bandwidth of the rectangular MS patch antenna in terms of its dimensions and substrate parameters is described in [25]. In [26], another simplified relation for quick calculation of BW (in MHz) for VSWR = 2 of the MS patch antenna operating at frequency f (in GHz), with h expressed (in cm) is derived. However, this simple formula does not take in account the dielectric constant of the patch antenna substrate and it can be only used for low-Q MS patch antenna with thin substrate.

Considering the average substrate permittivity expression in Eq. (1), Kumprasert et al. [27] developed a closed-form expression for the bandwidth in a prob-fed microstrip patch antenna. Following the bandwidth behavior, Parizi [28] described techniques to improve the bandwidth in MSPA. Among them, the intrinsic techniques aim to modify the antenna geometry, i.e. substrate thickness (h) and dielectric constant (ε_r), according to what was discussed in the prior paragraph. However, the author mentions that the counterpart of making an increase of h and decreasing ε_r affects the gain, increase the cross-polarization level and the spurious radiations. Therefore, not only geometry optimizations would be necessary to usefully increase the bandwidth, but also selecting the appropriate feeding technique and material dimensions that support the feeding. Referring particularly to the PC-MSPA, Parizi describes that the typical bandwidth ratio is about 8%, and an increase of this parameter can be obtained if increasing the thickness of the feeding layer, but being aware that more spurious radiation can be released. Another way to increase the bandwidth suggested is to make a matching structure in the port, i.e. a quarter-wave transformer between the input and the section that makes the coupling with the patch. In addition, other techniques have been used to enhance the bandwidth of electromagnetically coupled microstrip patch antennas by utilizing a tuning stub. In [19], a small tuning stub is connected in shunt with the feed line of the proximity coupled microstrip patch antenna to improve the impedance bandwidth. The similar approach with a dual-stub design has been used to increase the bandwidth from 4.8 to 8.4% in [29].

III. PROPOSED DESIGN MODEL FOR THE PC-MSPA

This section describes a new set of equations derived based on non-linear regression procedure to estimate the bandwidth of the PC-MSPA, shown in Fig. 1. The antenna PC-MSPA is designed to operate at f_o, where the MS transmission line is used to excite the MS patch is located between the patch substrate and the feeding substrate. From Fig. 1, the respective thickness and relative permittivities are h_1, ε_1, h_2 and ε_2, from which the rest of dimensions can be obtained. From these dimensions, and assuming ε_1=ε_2=ε_r, the following variables are also defined in terms of guided wavelength (λ_r=$\lambda_o/\sqrt{\varepsilon_r}$), $h_{1_{\lambda_r}}$=h_1/λ_r, R_h=h_2/h_1, and R_p=L_0/L_p, which will be used in the model equations following later in this section. The following new model equations (3-29) of R_p, R_h and $\%BW$ are obtained by applying the non-linear curve-fitting technique [30] to the full wave solutions.

A. GEOMETRY OF THE PC-MSPA

The PC-MSPA design procedure aims to get the complete antenna geometry (substrates thicknesses, patch and feed transmission line dimensions) from the knowledge of the material (relative permittivity ε_r) and desired central frequency (f_o).

1) Feed transmission line

It is known that the impedance matching is produced by having a feeding transmission line with the appropriate width and length, since these dimensions are directly related to the characteristic impedance and electrical length, respectively.

The transmission line width W_f can be set following the microstrip line design procedure [31] to get characteristic impedance Z_0 of 50 Ω, as Z_0=$f(W_f/h_1,\varepsilon_r)$.

On the other hand, the length L_f can be calculated as:

$$L_f = 0.5(L_g - L_p) + R_p L_p \quad (2)$$

The antenna matching can be set around the operating central frequency f_o if the length portion of the feeding transmission line L_0 is a certain fraction of the patch length L_p. In that sense, the fraction R_p can be calculated through the equations bellow and according to Fig. 1. These equations are illustrated in Fig. 2(a) with HFSS-simulated data and using the materials: Rogers™ 5880 Duroid (ε_r=2.2), Rogers™ 4350B (ε_r=3.66) and Rogers™ 6006 (ε_r=6.15).

$$R_p = x_1\ h_{1_{\lambda_r}}^3 + x_2\ h_{1_{\lambda_r}}^2 + x_3\ h_{1_{\lambda_r}} + x_4 \quad (3)$$

where x_1, x_2, x_3 and x_4 can be obtained using:

$$x_1 = 73.75\varepsilon_r^2 - 834.9\varepsilon_r + 3129 \quad (4)$$

$$x_2 = -149.9 - 257.1e^{-0.1708\varepsilon_r^2} \quad (5)$$

$$x_3 = 0.2772\varepsilon_r^2 - 2.489\varepsilon_r + 8.502 \quad (6)$$

$$x_4 = 0.89 \quad (7)$$

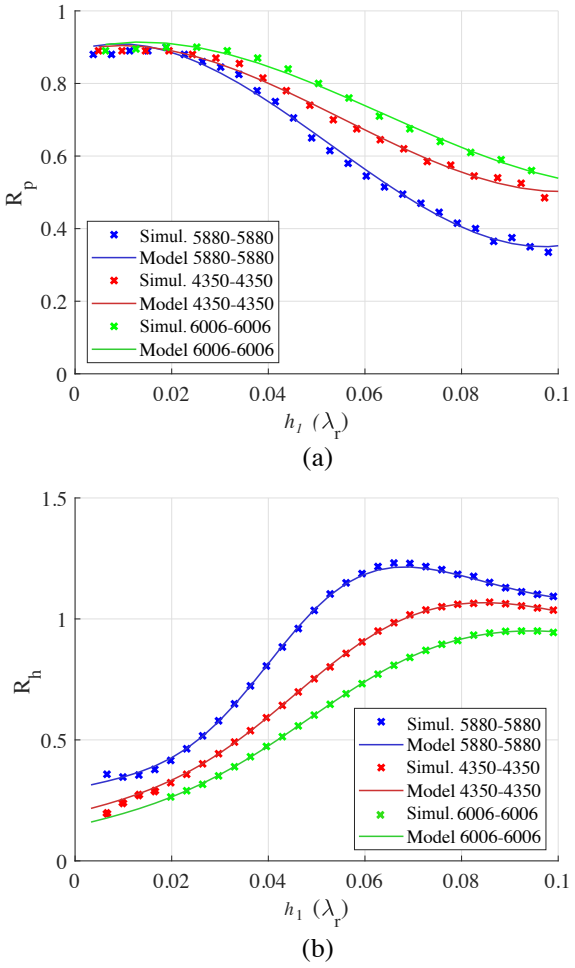

FIGURE 2: Comparison between the estimated and simulated values of: (a) R_p, and (b) R_h.

These equations are mostly valid for permittivities between 2.2 and 6.15, and with feed substrate thickness less than $0.1\lambda_r$ (265 mils in Rogers™ 5880 Duroid, 205 mils in Rogers™ 4350B, and 158 mils in Rogers 6006™ all at 3 GHz). In all the cases, it has been verified that W_f<W_p and W_f<$0.25\lambda_r$ when simulating the antenna geometry at S-band (2-4 GHz).

From the above equations and Fig. 2(a), it is found that the length of the feeding transmission line is more than half of the antenna length, and it tends to reduce as thicker are the substrates. It is also observed that the slope, thus R_p change per $h_{1\lambda_r}$ length unit, is decreased as the permittivity is increased. In order to eventually work in a dual port with differential feeding, R_p should be less than 0.5, that can happen at thicker substrates as lower permittivities have the feed substrate.

2) Total substrate thickness

The total thickness h_T=h_1+h_2 of the antenna in its optimum configuration can be calculated as:

$$h_T = h_1\left(1+\frac{h_2}{h_1}\right) = h_1(1+R_h) \tag{8}$$

Where the ratio R_h, which quantifies the relationship between the patch substrate thickness (h_2) and the feed substrate thickness (h_1) for maximizing bandwidth, can be modeled through the equations bellow. Fig. 2(b) provides an illustration of these equations.

$$R_h = y_1 + y_2\tanh\left(y_3(h_{1_{\lambda_r}} - y_4)\right) + y_5\cos\left(y_6\ h_{1_{\lambda_r}}\right) \tag{9}$$

where y_1, y_2, y_3, y_4, y_5 and y_6 can be obtained using:

$$y_1 = 1.379e^{-0.7\varepsilon_r} + 0.3682 \tag{10}$$
$$y_2 = 0.5182e^{-0.4078\varepsilon_r} + 0.6912 \tag{11}$$
$$y_3 = 128e^{-0.925\varepsilon_r} + 25.4 \tag{12}$$
$$y_4 = -0.0446e^{-0.6077\varepsilon_r} + 0.05295 \tag{13}$$
$$y_5 = 0.2694e^{-0.15\varepsilon_r} + 0.2903 \tag{14}$$
$$y_6 = 96.43e^{-0.9577\varepsilon_r} + 16.98 \tag{15}$$

Regarding the variations of this ratio over different relative permittivities, it is noticed that the majority of cases get the best coupling as R_h<1, thus h_2<h_1. Notice that the actual h_2 used in a design may be more or less than h_1, R_h, but the coupling would be reduced, affecting mainly the bandwidth. Besides, this ratio can get a maximum value, and this peak is inversely dependent on the permittivity, but once again, these cases where h_2>h_1 are only possible if ε_r<5.38, according to the presented equations. It is important also to observe that it can get a value equal to one (thus, h_2=h_1) as lower permittivities have both layers, which may be helpful in fabrication and logistics. As it is observed so far, this work contributes with the completion of the design of a PC-MSPA through the closed forms of the patch substrate thickness and the feeding structure dimensions.

3) Patch dimensions

The square patch can be initially designed from the rectangular patch dimensions (L_{po},W_{po}) as a start point. These initial dimensions can be obtained from [5] considering the total thickness h_T from Eq. 8, and then, the patch dimensions can be squared by making W_p=L_p=W_{po}.

B. CLOSE FORM FOR THE PC-MSPA BANDWIDTH

The impedance bandwidth is normally defined as the range of frequencies f_l (lower freq.), f_u (upper freq.) over which the return loss is acceptable (typically more than 10 dB ($|S_{11}|$<-10 dB)). However, the percentage (fractional) bandwidth is determined by the ratio between the impedance bandwidth and the central frequency f_c. Then, the percent-

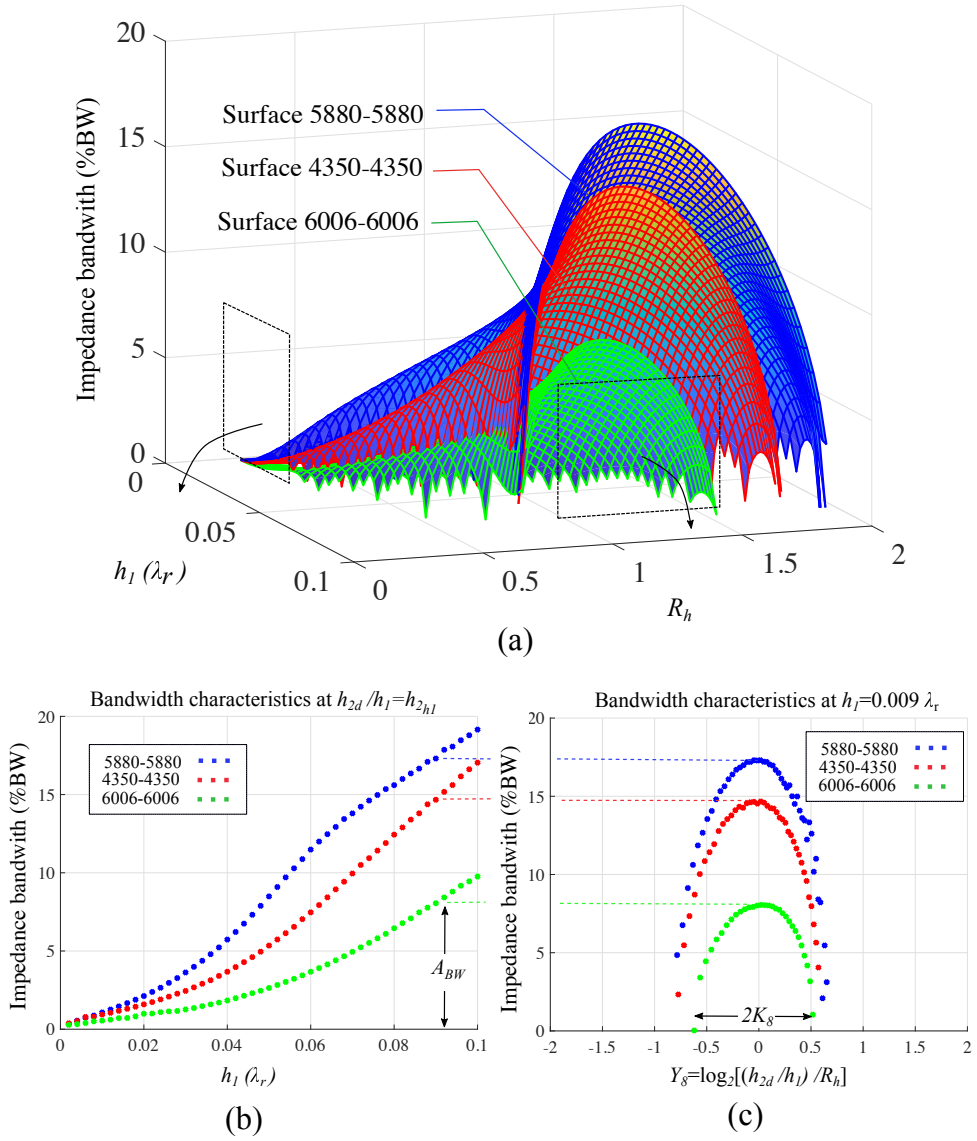

FIGURE 3: Bandwidth model and its side view projections, from where the terms A_{BW}, Y_8 and K_8 are illustrated.

age bandwidth is defined as:

$$\%BW = 100\frac{f_u - f_l}{f_c} = 200\frac{f_u - f_l}{f_u + f_l} \tag{16}$$

It can be estimated from the substrates thicknesses and relative permittivities, considering that the patch and the transmission line feed are set to match the designed frequency (L_0=R_p L_p, $f_c \approx f_\circ$). Then, the percentage bandwidth of the PC-MSPA with linear polarization can be predicted to be:

$$\%BW = A_{BW}\sqrt{1 - \frac{Y_8^2}{K_8^2}} \pm \Delta\%BW \tag{17}$$

Considering that the design assumes feed substrate with thickness h_1 and patch substrate with thickness h_{2_d}, where h_{2_d}/h_1 can be different from R_h of Eq. (9), and assuming equal permittivities (ε_1=ε_2=ε_r). Then, each term of Eq. (17) is expressed as:

$$A_{BW} = a_1\left[h_{1_{\lambda_r}}^2 - \frac{1}{2}\left(1 + \tanh\frac{h_{1_{\lambda_r}} - a_2}{10^{-3}}\right)(h_{1_{\lambda_r}} - a_2)^2\right] \tag{18}$$

where a_1, a_2, K_8 and K_a can be obtained using:

$$a_1 = 98840e^{-2.145\sqrt{\varepsilon_r}} + 533.6 \tag{19}$$

$$a_2 = -0.3252e^{-0.8037\sqrt{\varepsilon_r}} + 0.1231 \tag{20}$$

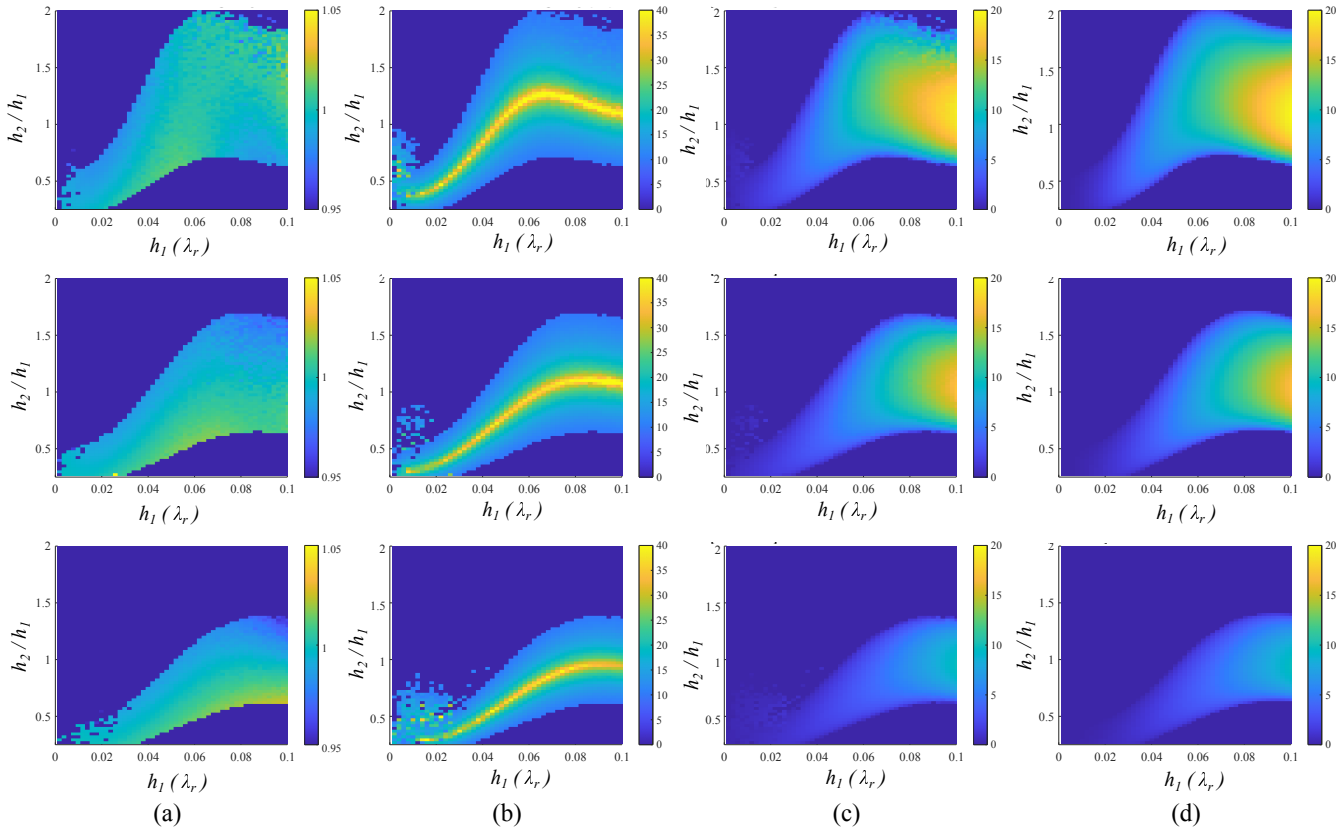

FIGURE 4: Antenna response for the PC-MSPA with different materials: Rogers™ 5880 Duroid (top row), Rogers™ 4350B (middle row) and Rogers™ 6006 (bottom row). All the variations are simulated at 3 GHz in $\lambda_\circ/2$ unit cell (L_g =5 cm). (a) Normalized central frequency, (b) Return loss at the central frequency (f_c), (c) Simulated percentage bandwidth, and (d) Modeled percentage bandwidth.

$$K_8 = \log_2 K_{BW} = \log_2 \left[\frac{K_a}{R_h} + \sqrt{4 + \left(\frac{K_a}{R_h}\right)^2} \right] - 1 \tag{21}$$

$$K_a = k_1 + k_2 \tanh(k_3(h_{1_{\lambda_r}} - k_4)) + k_5 \cos\left(k_6\ h_{1_{\lambda_r}}\right) \tag{22}$$

where k_1, k_2, k_3, k_4, k_5, k_6, and Y_8 can be obtained using:

$$k_1 = 0.7682e^{-0.3526\varepsilon_r} + 0.4086 \tag{23}$$
$$k_2 = 2.299e^{-0.5975\varepsilon_r} + 0.2538 \tag{24}$$
$$k_3 = 80.32e^{-1.028\varepsilon_r} + 42.36 \tag{25}$$
$$k_4 = -0.06715e^{-0.771\varepsilon_r} + 0.04963 \tag{26}$$
$$k_5 = 1.271e^{-0.5736\varepsilon_r} + 0.07257 \tag{27}$$
$$k_6 = 311.6e^{-1.406\varepsilon_r} + 18.96 \tag{28}$$

$$Y_8 = \log_2 \left(\frac{h_{2_d}/h_1}{R_h} \right) \tag{29}$$

The equations expressed above for estimating the percentage bandwidth of the PC-MSPA can be summarized in three components: bandwidth amplitude A_{BW}, substrate allowable range K_8, and normalized substrate thickness ratio Y_8. The graphical representation of these equations are illustrated in Fig. 3. Also, there is a term of error $\Delta\%BW$, which is analyzed with more detail in Section V.

As a consequence, the formula of the bandwidth of Eq. (17) could be modeled as family of semi-elliptical curves, where the families are conformed by $h_{1_{\lambda_r}}$ variations and each semi-ellipse has a height A_{BW}, a width $2K_8$, and they are centered in Y_8.

Further than the mathematical representation, the equations may be physically interpreted as the permittivities and substrate thickness change. As the permittivity increases, the bandwidth tends to reduce, and it is observed in the A_{BW} term, which also has a quadratic-linear growth as the feeding substrate becomes thicker. Meanwhile, K_8 which mathematically is interpreted as a shape parameter represents the range of substrate thicknesses ratio where a bandwidth can exist. Lastly, but not less important, Y_8 represent the deviation of substrate ratio from R_h. Therefore, if an antenna with certain feeding substrate thickness h_1 has patch substrate thickness h_{2_d}=$h_1 R_h$, then it would have the maximum bandwidth, as Y_8=0. Notice that K_8 and Y_8 are in logarithmic space (octaves) and not in arithmetic progression.

IV. IMPLEMENTATION, MEASURED RESULTS AND VALIDATION

Full wave simulations of the antenna of Fig. 1 were performed at f_o=3 GHz, considering three different materials and changing h_1 from 0.002 λ_r to 0.1λ_r, h_2 from 0.275h_1 to 2h_1. The transmission line length was calculated according to Eq. 2, where R_p was obtained and calculated in Eq. 3. The results are shown in Fig. 4, as follows: the first column describes the normalized central frequency (f_c/f_o) that in the best case should be 1; the second column shows the return loss at the simulated value of f_c=$(f_u + f_l)/2$ where $[f_l; f_u]$ is the interval where $|S_{11}|$<-10 dB; and then the third and fourth columns display the simulated and modeled percentage bandwidth of Eq. (16) and Eq. (17), respectively. For the three different materials, the model results of the percentage bandwidth in Fig. 4(d) are in good agreement with the corresponding simulated ones shown in Fig. 4(c).

On the other hand, four antenna configurations have been fabricated and measured, using two different materials and different design frequencies in the S, C and X bands. These cases have been labeled as 'Case 1', 'Case 2', 'Case 3' and 'Case 4', which specifications are listed in Table 1, noticing that R_h=1 in all the cases. The simulated and measured reflection coefficients in (dB) of these antennas are shown in Fig. 5. The antenna in Case 1 and Case 4 has a ground plane size of $\lambda_o/2$ x $\lambda_o/2$ where λ_o is the free space wavelength of the design frequency. However, it is important to mention that the ground plane in the antennas of Case 2 and Case 4 has been extended to 5 cm ($\lambda_o/2$ at 3 GHz), in order to facilitate the connections for measurements. From Fig. 5, it is clear that the measured results mostly agree and validate the results produced via simulations for all cases. A small discrepancy between the simulated and measured results may be caused by the error of the fabrication and assembling of the antenna.

Furthermore, an analysis of model errors is presented through the plots in Fig. 6. The plot in Fig. 6(a) shows the percentage RMSE error of the central frequency in the simulation results with respect to the intended central frequency, which is expressed as $\Delta f_c/f_c$. Meanwhile, Fig. 6(b) shows the bandwidth error term in Eq. (17), which is calculated as $\Delta\%BW$=$|\%BW_{modeled} - \%BW_{simulated}|$ from Fig. 4.

TABLE 1: Fabricated antennas' specifications.

Parameters	Units	Case 1	Case 2	Case 3	Case 4
f_o	GHz	3	6	6	10
$\varepsilon_1, \varepsilon_2$	-	2.20	3.48	3.48	2.20
h_1, h_2	mm	3.175	1.524	1.524	0.790
L_p, W_p	mm	29.40	11.82	11.80	9.070
L_g, W_g	mm	50.00	50.00	2.000	50.00
R_p	-	0.686	0.687	0.721	0.760
L_f	mm	27.87	13.27	12.68	11.50
W_f	mm	10.00	3.350	3.350	2.420
L_s	mm	1.800	1.500	1.500	1.500
L_o	mm	20.56	7.680	7.100	4.530

V. ERROR ANALYSIS

Table 2 quantifies the errors between simulated, measured with calculated results using the proposed method described in Section III. For all cases this error analysis was performed using the central frequency (f_c) and frequency band (BW) for each prototype.

TABLE 2: Errors between the proposed model and both simulation and measurement.

Case	f_c	$\%(\Delta f_c)/f_c$		$\Delta\%BW$	
		Measured	Simulated	Measured	Simulated
Case 1	3 GHz	0.17	0.04	1.41	0.18
Case 2	6 GHz	1.91	0.99	0.80	0.98
Case 3	6 GHz	0.09	0.76	0.15	1.46
Case 4	10 GHz	1.00	1.30	0.65	0.39

The central frequency in all simulated cases are around the design operation frequency, having an root mean square error (RMSE) less than 5% (1.34% in Rogers 5880, 1.45% in Rogers 4350, and 2.76% in Rogers 6006), as noticed in the color space in the first column of Fig. 4. This high agreement is due to the accurate design from Eq. (2). However, in the same figure, it is seen that for very thin antennas (h_1<$0.03\lambda_r$, h_{2d}/h_1<0.75), the normalized central frequency f_c/f_o is less than 0.95 (dark blue colored in the first column that are not in the other columns), reflecting also in the higher RMSE as shown in Fig. 6(a). These fluctuations are primarily due to the numerical simulation errors for very thin substrates. On the other hand, as the feed thickness h_1 increases (h_1>$0.03\lambda_r$), the percentage RMSE go down to less than 5%. Meanwhile, according to Table 2, the measured central frequency in the four cases also have a very good agreement, having slightly more errors in Case 2 and Case 4, due to fabrication imperfections.

The maximum return loss, and maximum predicted bandwidth, are obtained when the parameter Y_8=0 in Eq. (17), which means h_{2_d}=$h_1 R_h$. This has been verified through the comparison between the simulations of Fig. 4(b) and the frequency responses of Fig. 5. Considering Case 1 and Case 3, which do not have a ground plane extension, the values of $|Y_8|$ are 0 and 0.17, meaning that the return loss would be stronger in Case 1 than in Case 3. This behavior is clearly observed in the simulation and experiment as shown in Fig. 5(a) and Fig. 5(c).

Regarding the antenna bandwidth, the RMSE of the term $\%\Delta BW$ is less than 2, as observed in Fig. 6(b), showing high accuracy of the model in comparison with the simulation. These errors remain the same over $h_{1_{\lambda_r}}$, but they represent a bigger relative error when $h_{1_{\lambda_r}}$ is small, i.e. less than $0.03\lambda_r$, being observed, e.g in the dusty area in the bottom-left image corners in the Fig. 4(b), where the predicted bandwidth is zero. Due to numerical fluctuations in the simulations, the term $\Delta\%BW$ may be higher at $Y_8 \approx K_8$, where the expected percentage bandwidth goes to zero. In addition, from the experimental results, it is observed in Table 2 that the bandwidth has an error term up to 1.46%. Overall, the expression of the bandwidth can

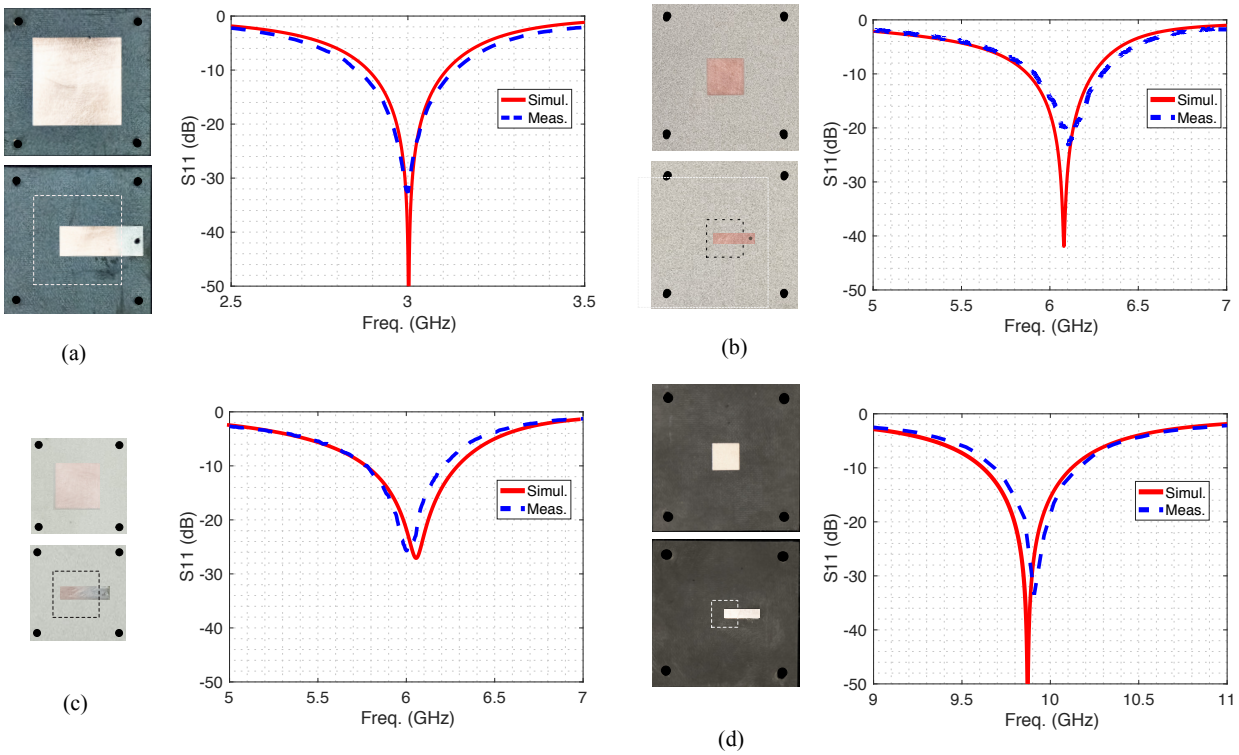

FIGURE 5: Measured and simulated $S11(dB)$ over frequency for: (a) Case 1: S-band PC-MSPA, (b) Case 2: C-band PC-MSPA, (c) Case 3: C-band PC-MSPA, and (d) Case 4: X-band PC-MSPA.

get a good estimation of the bandwidth, but it should be considered only as a reference value, as it may differ from measured values due to fabrication errors and limitations, as well as numerical errors especially in very thin antennas.

Those results mean that the proposed model of R_p allows to have a PC-MSPA with an stabilized central frequency and around the design frequency of the antenna. The maximum return loss and bandwidth results show that the model and prediction have good agreement with results, but the model errors may increase as more modifications the antenna has, and as h_{2_d}/h_1 is far away from the R_h, affecting the maximum return loss and bandwidth as well. In that sense, in order to increase the bandwidth, it is observed that feed substrates with higher thickness would allow to reach this purpose, as long as the patch substrate has the appropriate dimension related to R_h in order to maximize coupling.

In addition, the proposed model is compared with other models available in literature [24], [25], [26]. The calculated percentage bandwidths for electrically thin and thick PC-MSPA antennas with different physical dimensions and substrates are compared with those from HFSS simulations and other models. Four cases of study are used and listed in Table 3, considering the simulated value of the PC-MSPA bandwidth as a reference. It is seen from Table 3 that when the substrate electrically thickness like Case 2 and Case 3, the error between the simulated and predicated bandwidth is less than 0.1% using the new model. However, as expected other models have higher errors; in some of them, the error

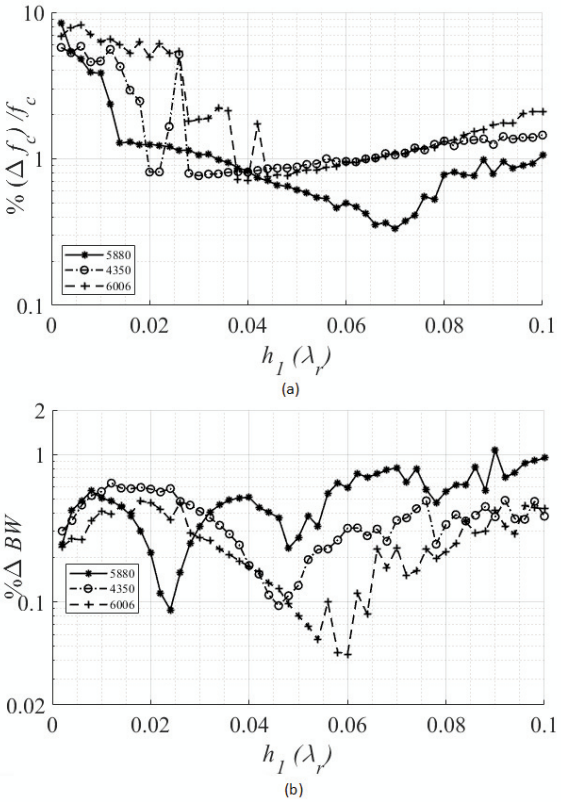

FIGURE 6: RMSE model errors over $h1_{\lambda_r}$: (a) Central frequency fluctuations, (b) Percentage bandwidth term $\%\Delta BW$.

TABLE 3: A comparison between the proposed model for PC-MSPA bandwidth and available models for MSPA bandwidth ($h_1 = h_2$, $L_p = W_p$).

Parameters	Reference (HFSS)	Bandwidth (Error)	Theoretical Bandwidth Estimation			
			Proposed Model	Previous Work		
				Ref. [24]	Ref. [25]	Ref. [26]
f_o=3 GHz, ε_r=2.20 h_1=125 mil, W_p=29.40 mm	7.430	$\%BW$ (Δ_{BW})	**(7.610)** **(0.180)**	6.433 (0.997)	7.706 (0.276)	9.600 (2.170)
f_o=10 GHz, ε_r=6.15 h_1=50 mil, W_p=4.85 mm	10.28	$\%BW$ (Δ_{BW})	**(10.37)** **(0.090)**	4.323 (5.959)	6.145 (4.317)	12.80 (2.518)
f_o=10 GHz, ε_r=3.48 h_1=60 mil, W_p=6.28 mm	16.38	$\%BW$ (Δ_{BW})	**16.32** **(0.060)**	7.963 (8.417)	10.89 (5.487)	15.36 (1.020)
f_o=6 GHz , ε_r=2.20 h_1=125 mil, W_p=12.19 mm	17.79	$\%BW$ (Δ_{BW})	**18.17** **(0.385)**	13.64 (4.149)	18.84 (1.052)	19.20 (1.415)

is about 10%. For electrically thin substrates, Case 1 and Case 4, the new model generally has better performance even though other models have comparable results.

VI. CONCLUSION

This paper has provided a new set of equations to compute the bandwidth of a proximity-coupled square microstrip patch antenna (PC-MSPA). The proposed model is used for two layers (thin or thick) PC-MSPA. A extensive mathematical analysis of this antenna has been undertaken at several levels of design complexity to evaluate the robustness of proposed expressions. Generic expressions used to calculate impedance bandwidth of edge and probe-fed microstrip patch antennas has been discussed and compared with proposed model. Although those expressions can be used for PC-MSPA, those does not provide accurate estimation of bandwidth of a PC-MSPA. Four PC-MSPA antennas were designed, fabricated with different materials, thickness, bandwidth requirements and frequency bands. In all cases, simulated and measured results agree very well with results obtained from proposed analytical model. Less than 3.1% are the errors when the proposed model is compared with simulated and measured results.

ACKNOWLEDGMENT

The authors like to thank the Advanced Radar Research Center at The University of Oklahoma for providing the facilities needed to perform this research. They would also like to thank all members of PAARD research group for the discussions and positive feedback at the weekly team meeting. This material is based upon work partially supported by the Office of Navy Research (ONR) under Grant No.1532140.

REFERENCES

[1] A. G. Deschamps, "Microstrip microwave antennas," Third USAF Symposium on Antennas, 1953.
[2] H. Gutton and G. Baissinot, "Flat aerial for ultra high frequencies," French Patent No. 703 113, 1955.
[3] R. E. Munson, "Conformal microstrip antennas and microstrip phased arrays," IEEE Trans. Antennas Propagat., vol. AP-22, no. 1, pp. 74–78, 1974.
[4] J. W. Howell, "Microstrip antennas," IEEE Trans. Antennas Propagat., vol. AP-23, no. 1, pp. 90–93, 1975.
[5] C. A. Balanis, Antenna theory : analysis and design. John Wiley & Sons, 2015.
[6] K. F. Lee, Microstrip Patch Antennas. Imperial College Press, London, 2011.
[7] P. Bhartia, I. Bahl, R. Garg, and A. Ittipiboon, Microstrip Antenna Design Handbook. Artech House, London, 2001.
[8] D. Pozar and D. Schaubert, Microstrip Antennas: The Analysis and Design of Microstrip Antennas and Arrays. IEEE Press, New York, 1995.
[9] K. R. Carver and J. W. Mink, "Microstrip antenna technology," IEEE Trans. Antennas Propagat., vol. AP-29, pp. 2–24, 1981.
[10] E. H. Van Lil and A. R. Van de Capelle, "Transmission line model for mutual coupling between microstrip antennas," IEEE Trans. Antennas Propagat., vol. AP-32, pp. 816–821, 1984.
[11] Y. T. Lo, D. Solomon, and W. F. Richards, "Microstrip microwave antennas," IEEE Trans. Antennas Propagat., vol. AP-27, pp. 137–145, 1979.
[12] W. F. Richards, Y. T. Lo, and D. D. Harrison, "An improved theory of microstrip antennas with applications," IEEE Trans. Antennas Propagat., vol. AP-29, pp. 25–27, 1981.
[13] V. Palanisamy and R. Garg, "Analysis of arbitrarily shaped microstrip patch antennas using segmentation technique and cavity model," IEEE Trans. Antennas Propagat., vol. 34, pp. 1208 – 1213, 1986.
[14] M. Davidovitz and Y. Lo, "Rigorous analysis of a circular patch antenna excited by a microstrip transmission line," IEEE Trans. Antennas Propagat., vol. 37, no. 8, pp. 949–957, 1989.
[15] M. Tsai, F. Flaviis, O. Fordham, and N. Alexopoulos, "Modeling planar arbitrarily shaped microstrip elements in multilayered media," IEEE Trans. Microwave Theory and Tech., vol. 45, no. 3, pp. 330–336, 1997.
[16] F. Alonso-Monferrer, A. kishk, and A. Glisson, "Greesn's functions analysis of planar circuits in a two-layer grounded medium," IEEE Trans. Antennas Propagat., vol. 40, no. 6, pp. 690–696, 1992.
[17] D. Pozar and S. Voda, "A rigorous analysis of a microstripline fed patch antenna," IEEE Trans. Antennas Propagat., vol. AP-35, no. 12, pp. 1343–1350, 1987.
[18] G. Splitt and M. Davidovitz, "Guidelines for design of electromagnetically coupled microstrip patch antennas on tow-layer substrate," IEEE Trans. Antennas Propagat., vol. 38, no. 7, pp. 1136–1140, 1990.
[19] D. M. Pozar and B. Kaufman, "Increasing the bandwidth of a microstrip antenna by proximity coupling," Electronics letters, vol. 23, no. 8, pp. 368–369, 1987.
[20] K. Lee, Fong, and K.-F. Tong, Microstrip Patch Antennas. Singapore: Springer Singapore, 2016, pp. 787–852.
[21] R. P. Parrikar and K. C. Gupta, "Multiport network model for cad of electromagnetically coupled microstrip patch antennas," IEEE Trans. on Antennas and Propagat., vol. 46, no. 4, pp. 475–483, April 1998.

[22] H. F. Pues and A. R. Van de Capelle, "An impedance-matching technique for increasing the bandwidth of microstrip antennas," IEEE Trans. on Antennas and Propagat., vol. 37, no. 11, pp. 1345–1354, Nov 1989.
[23] M. P. David, D. Pozar, and D. Schaubert, "A review of bandwidth enhancement technique for microstrip antennas," in Microstrip Antennas: the analysis and design of microstrip antennas and arrays. IEEE press, 1995, pp. 157–166.
[24] D. R. Jackson and N. G. Alexopoulos, "Simple approximate formulas for input resistance, bandwidth, and efficiency of a resonant rectangular patch," IEEE Trans. on Antennas and Propagat., vol. 39, no. 3, pp. 407–410, March 1991.
[25] G. Kumar and I. Ray, Broadband Microstrip Antennas. Artech House, London, 2003.
[26] R. C. Johnson, Antenna Engineering Handbook. New York: McGraw-Hill, 1993.
[27] N. Kumprasert, C. Namkang, and T. Tassri, "Parametric study of the rectangular microstrip antenna with an air gap," in R & D Journal, Bangkok, vol. 24, 2001, pp. 131–142.
[28] a. S. A. R. Parizi, "Bandwidth enhancement techniques," in Trends in Research on Microstrip Antennas. InTech, nov 2017.
[29] S. M. Duffy, "An enhanced bandwidth design technique for electromagnetically coupled microstrip antennas," IEEE transactions on antennas and propagation, vol. 48, no. 2, pp. 161–164, 2000.
[30] S. L. Arlinghaus, Practical Handbook of Curve Fitting. CRC Press, 1994.
[31] R. Garg, I. Bahl, and M. Bozzi, Microstrip Lines and Slotlines. Artech House, 2013.

NAFATI ABOSERWAL (S'13-M'16) received the B.S. degree in Electrical Engineering from Al-Mergheb University, Alkhoms, Libya, in 2002. He received his M.S. and Ph.D. degrees in Electrical Engineering from Arizona State University, Tempe, AZ, in 2012 and 2014, respectively. In January 2015, he joined the Advanced Radar Research Center (ARRC) and the Department of Electrical and Computer Engineering at The University of Oklahoma (OU), Norman, as a Postdoctoral Research Scientist. Currently he is a Research Associate and a Manager of Far-Field, Near-Field and Environmental Anechoic Chambers at the Radar Innovations Laboratory (RIL). His research interests include EM theory, computational electromagnetics, antennas, and diffraction theory, edge diffraction and discontinuities impact on the array performance. His research also focuses on active high performance phased array antennas for weather radars, higher modes and surface waves characteristics of printed antennas, and high performance dual-polarized microstrip antenna elements with low cross-polarization. Dr. Aboserwal is a member of the IEEE Transactions on Antennas and Propagation.

NIM R. CCOILLO RAMOS got the B. Sc and M. Sc degrees in Electronics Engineering from Universidad Nacional de Ingenieria (UNI, Lima-Peru) in 2016 and 2018, respectively. At the end of his undergraduate studies, he joined in the National Institute of Research and Training in Telecommunications (INICTEL-UNI, Lima-Peru), working as an intern in Electronics Engineering with focus on Electromagnetics and after graduate studies, as a research assistant. During his graduate studies, he worked in X-and-P-band radar image processing to estimate forest changes in the Amazon, having a six-month stay at the Department of Telecommunications of the State University of Campinas, Brazil. Since January 2019, he has been pursuing the PhD program in Electrical and Computer Engineering at the University of Oklahoma (OU), USA, researching in electromagnetic antenna modeling for phased arrays in the Advanced Radar Research Center at OU.

ZEESHAN QAMAR (S'11-M'17) received the B.Sc. and M.Sc. degrees in electrical engineering from the COMSATS University, Islamabad, Pakistan, in 2010 and 2013, respectively, and the Ph.D. degree in electronic engineering from the City University of Hong Kong, Hong Kong, in 2017. From Jul. 2010 to Aug. 2013, he was a Research Associate with the Department of Electrical and Computer Engineering, COMSATS University. From Nov. 2017 to Apr. 2018, he was a Postdoctoral Research Associate with the Department of Materials Science and Engineering, City University of Hong Kong. He is currently a Post- Doctoral Research Fellow with the Phased Array Antenna Research and Development group (PAARD) and the Advanced Radar Research Center (ARRC) at The University of Oklahoma, Norman, OK, USA. His current research interests include microwave/millimeter-wave circuits, material characterization, meta-materials, artificial dielectric layer, antennas and phased arrays, phased array antennas. He is a member of the IEEE Antennas and Propagation Society (AP-S), and a reviewer of various IEEE and IET conferences and journals.

JORGE L. SALAZAR-CERRENO (S'00-M'12-S'14) received a B.S. In ECE from the University Antenor Orrego, Trujillo, Peru, M.S. degree in ECE from the University of Puerto Rico, Mayagüez (UPRM). In 2011, he received his Ph.D. degree in ECE from the University of Massachusetts, Amherst. His Ph.D. research focused on development of low-cost dual-polarized active phased array antennas (APAA). After graduation, Dr. Salazar-Cerreno was awarded a prestigious National Center for Atmospheric Research (NCAR) Advanced Study Program (ASP) postdoctoral fellowship. At NCAR, he worked at the Earth Observing Laboratory (EOL) division developing airborne technology for two-dimensional, electronically scanned, dual-pol phased array radars for atmospheric research. In July 2014, he joined the Advanced Radar Research Center (ARRC) at The University of Oklahoma as a research scientist, and became an assistant professor at the School of Electrical and Computer Engineering in August 2015. His research interests include high-performance, broadband antennas for dual-polarized phased array radar applications; array antenna architecture for reconfigurable radar systems; APAA; Tx/Rx modules; radome EM modeling; and millimiter-wave antennas. In 2019, Dr. Salazar was awarded the prestigious William H. Barkow Presidential Professorship from The University of Oklahoma for meeting the highest standards of excellence in scholarship and teaching. Dr. Salazar is He is a senior member of the IEEE Antennas and Propagation Society (AP-S), and a reviewer of various IEEE and AMS conferences and journals.